

# Histogramming algorithm for muon standalone reconstruction in the CMS detector

Troy Mulholland  
Department of Physics  
St. Bonaventure University  
University of Florida REU participant: Summer, 2009

Mentored by:  
Ivan Furic Ph.D.  
Department of Physics  
University of Florida

## Abstract:

The Large Hadron Collider (LHC) at the European Organization for Nuclear Research (CERN) in Geneva, Switzerland is set to begin this Fall. One of the first physics results expected from the new collider is a search for massive, TeV-range resonances decaying to di-muons and di-electrons. At high momentum, a muon will exhibit electromagnetic showering. The present muon reconstruction algorithms can be easily confused by additional detections generated in the shower. We propose a histogramming algorithm to account for the additional showering effects. To define a muon algorithm, we have to demonstrate a method for finding detections belonging to the muon, and provide initial estimates of the muon direction and momentum for detailed fitting. We present studies of both the algorithm for the central part of the Compact Muon Solenoid (CMS) detector at the CERN LHC. The muon  $\phi$  angle change through the detector has been found to be exponential as a function of decreasing momentum. This seed will need to be put into a fitter for future studies of muon momentum using this algorithm. Moreover, a similar study can be done in the endcap region of the detector.

## Introduction:

The two main particle detectors for the Large Hadron Collider at CERN are A Toroidal LHC Apparatus (ATLAS) and CMS. The CMS detector's two main components consist of a barrel region and an endcap region. In the barrel region muons are detected using Drift Tubes (DTs), while the endcap region detects muons using cathode strip chambers (CSCs). The CMS detector also features a 4T solenoid to properly identify particles. The CMS barrel region is

separated into wheels that are cross sections of the barrel along its length, sectors that divide the wheel into twelve roughly equally spaced wedges, and four stations in each sector that house the muon detecting layers. Iron absorbers separate the stations. Inside the muon detectors are a hadron calorimeter and an electromagnetic calorimeter [1]. Only muons and neutrinos are likely to pass through the calorimeters and iron shielding. Since the muon detectors can only detect charged particles, neutrinos will pass through without detection.

Drift Tubes are organized into layers, super layers, and stations. A Drift Tube is a long hollow tube with a wire running along its center. A high potential and a gas exists between the wire and the drift tube enclosure. When a charged particle such as a muon travels through the gas, the muon knocks electrons off the atoms in the gas. The potential difference between the drift tube walls and wire creates a small detectable current [2]. These drift tubes compose the drift tube layers. There are four drift tube layers in each super layer. The wires in the first and third super layer in each station run parallel to the particle beam allowing for measurement in the  $\rho$ - $\phi$  coordinate plane. The wires in the middle super layer of each station run perpendicular to the particle beam allowing for measurement in the  $\rho$ - $z$  coordinate plane.

Previous muon track reconstructing methods provide accurate results under most circumstances; however, they fail to account for unusual muon behavior at the highest energies that will be produced at the LHC. The purpose of my project is to develop a histogramming algorithm to locate the track of a muon with high energies through the barrel region. For highly energetic muons, there exists an effect called particle showering. A shower happens when a highly energetic charged particle, in our case a muon, travels through a dense medium. While in the dense medium, it is typical that the muon will exhibit bremsstrahlung which means the muon will emit a highly energetic photon. At the LHC, the loss in energy of the muon due to

bremsstrahlung is comparatively insignificant. However, this emitted photon is energetic enough to exhibit pair production. In pair production, the photon interacts with the nucleus of an atom and creates an electron positron pair [3]. Since the DTs are designed to detect charged particles, electrons and positrons will also register hits. These hits disrupt muon tracking methods because of the disordered drift tube detections. Below are two separate events being in CMSShow Fireworks, a visualization package that allows one to import one's own Monte Carlo files. Figure 1 displays a clean, non-showering muon while Figure 2 displays an example of a muon that is exhibiting particle showering. The view in these figures is along the z axis of the detector seeing the the  $\rho$ - $\phi$  coordinate plane. The highlighted stations have registered detections with the dashed lines being the DT detections themselves.

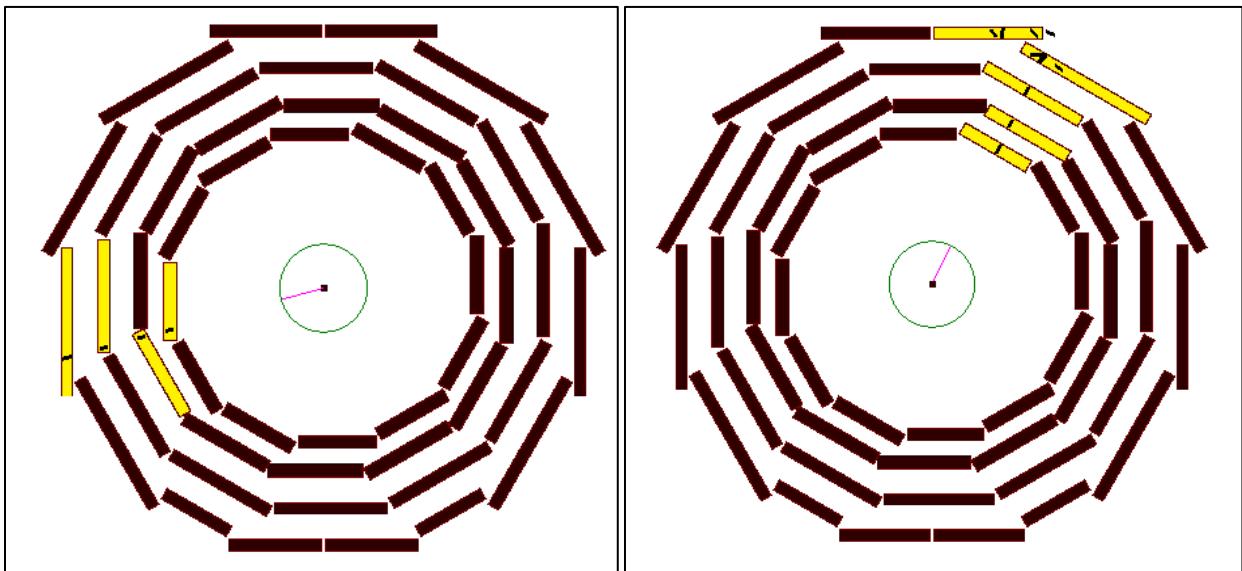


**Figure 1: Non-showering muon**

**Figure 2: Showering muon**

Our approach to the problem is the following. Since the muon is highly energetic, it should not bend much while in the DT layers. Using this basis we reconstructed an algorithm that uses a  $\chi^2$  method to map the DT hits. This mapping produces a spike in the direction of the

muon trajectory regardless of muon showering.

To implement this algorithm, we must put the data into a fitter. We have produced a seed for the fitter by checking the change in  $\phi$  angle between the muon stations at a range of transverse momentum between 300 GeV and 1 TeV. Transverse momentum, abbreviated as  $P_t$ , is the component of the momentum that is transverse to the beamline of the particle detector. We also checked how the angle in the  $\rho$ - $z$  plane would affect the  $\Delta \phi$  data. This was measured in  $\eta$  which will be described more thoroughly later in the paper.

## Method:

This algorithm was written in C++ with the CMS Software (CMSSW) and ROOT for analyzing data. Within CMSSW the coordinate systems at our disposal are global cartesian coordinates and cylindrical coordinates with the origin at zero. The  $z$  axis runs parallel to the beamline of the detector. Also, there is local, one dimensional DT coordinates that measure the distance from a given DT wire to a detection in the DT. One problem to overcome is that the DT only identifies the distance away from the origin and cannot distinguish whether the hit was in the positive direction or negative direction. Previous reconstruction algorithms account for this by simply connecting only the detections that make a straight line, thus eliminating false detections. This algorithm fails, however, when a shower occurs because the disordered DT detections allow for many straight line configurations.

The first step in this process is to map the DT detections in both  $\rho$ - $\phi$  and  $\rho$ - $z$ . Figure 3 shows all super layer 1 and 3 detections in the  $\rho$ - $\phi$  plane for a single event while Figure 4 shows all super later 2 detections in the  $\rho$ - $z$  plane for a single event.

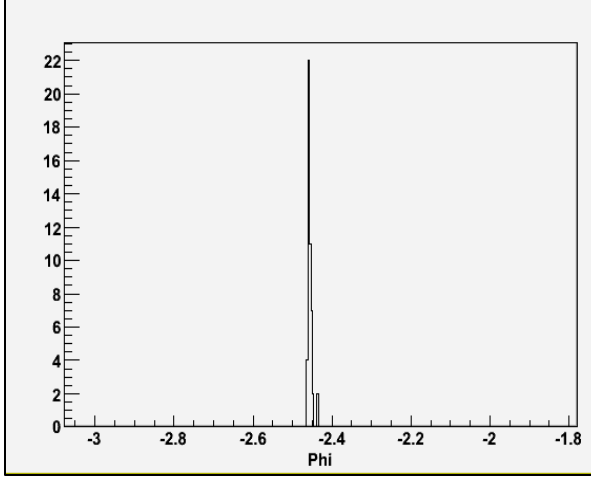


**Figure 3: raw  $\phi$  detections**

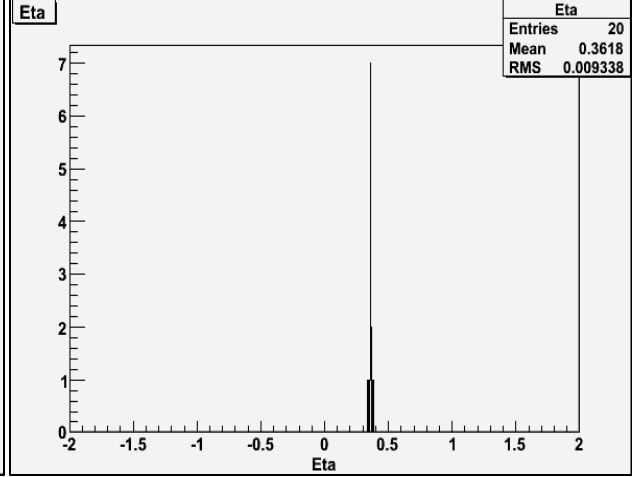


**Figure 4: raw  $\eta$  detections**

$\rho$  - $\phi$  detections are registered in  $\phi$  from  $-\pi$  to  $\pi$  and  $\rho$ -z detections are measured in  $\eta$  with  $\eta$  being:

$$\eta = -\ln \tan \frac{\theta}{2} \quad (1)$$

and  $\theta$  being the angle between the transverse momentum of the muon and the beamline of the colliding particles. This is known as pseudorapidity. For the CMS any  $\eta$  values between -1.0 and 1.0 will be registered in the DTs, all others will be registered in the CSCs.

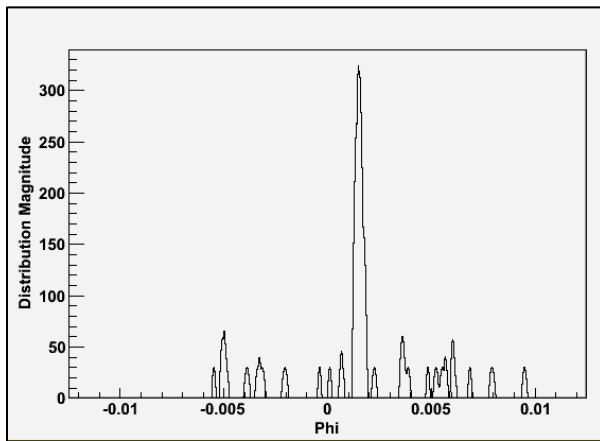
Our Algorithm takes this data to narrow our focus to a range of 10 cm plus and minus the location where the maximum number of detections were registered. Once this is done, we apply a  $\chi^2$  distribution to the hits:

$$\chi^2 = \frac{(X-\mu)^2}{\sigma^2} \quad (2)$$

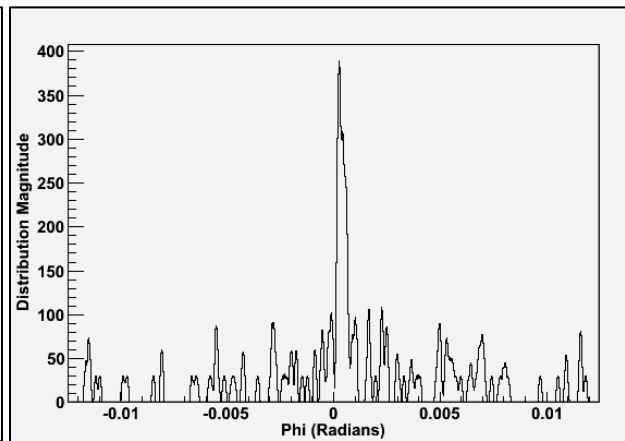
where  $X$  is the location of the detection,  $\mu$  is the distance from the detection and  $\sigma$  is  $\frac{150 \mu\text{m}}{\rho}$ .

This distribution is then plotted if it satisfies the condition that  $30 - \chi^2 > 0$ . Figure 5 shows a typical event with little noise. In this particular event, no showering was visible. Figure 6

displays an event where a known shower is present. As illustrated, though there is a larger amount of noise, a spike still exists in the direction of if the muon. Moreover, the spike is actually larger than the spike in the non-showing event. This is because showering particles do not affect the muon greatly, and the spike magnitude depends on only the number of detections registered.



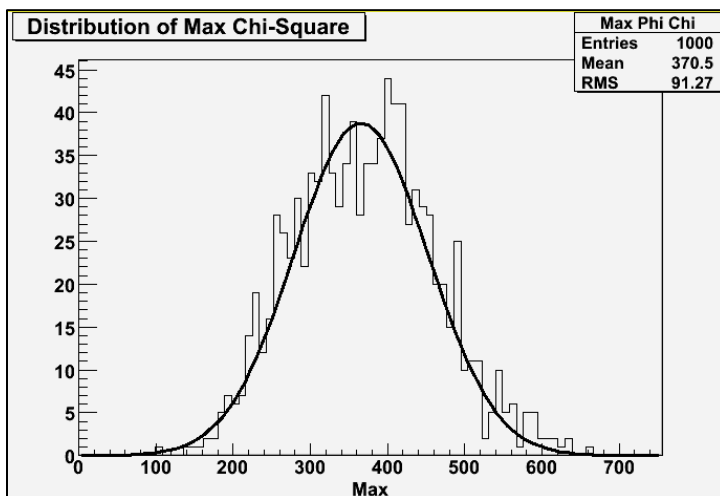
**Figure 5: non-showering muon**



**Figure 6: showering muon**

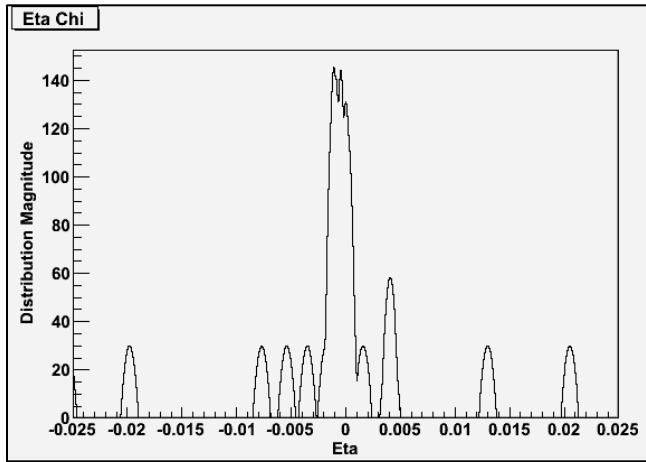
A good height of the spike for accurate data ranges with spikes of magnitude 200 or higher. These events would provide enough certainty that the muon shows over the background noise.

Figure 7 shows the  $\chi^2$  maxima for 1000 events. This data fit with a normal distribution yields a



**Figure 7:  $\chi^2$  Maxima Distribution**

mean of 370.5 and a standard deviation of 91.27. This tells us that 96.9% of the plots recorded a maximum larger than 200.



**Figure 8:  $\chi^2$  Distribution in  $\eta$**

Figure 8 shows the application of the same algorithm in the  $\rho$ -z plane, instead of the  $\rho$ - $\phi$  plane. The processes parameters are the same except there will be fewer detections because there is only one super layer per station that will register detections in  $\eta$  vs. two super layers per station that will register detections in  $\phi$ .

### Results:

In order to do further analysis using this algorithm, one must put this data into a fitter; however, the fitter must first be seeded. To seed this algorithm, we needed to know the bending magnitude at different momentum due to the external magnetic field. A seed is a rough estimate of the particles direction and momentum. Momentum can be determined from the deflection angle between stations. To do this we first fit the detections in each station with a linear regression. Once this was accomplished we could compare the change in  $\phi$  from station to station. Figure 9 shows the  $\Delta \phi$  between the first detection in station 1 and the last detection in station 2. Figure 10 shows  $\Delta \phi$  between station 1 and 3, and Figure 11 shows  $\Delta \phi$  between station 3 and 4. These plots were filled with data samples of muons with Pt of 1 TeV.

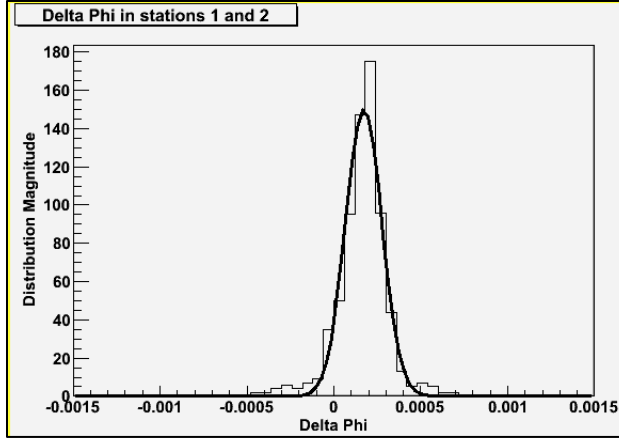


Figure 9:  $\Delta \phi$  between stations 1 and 2

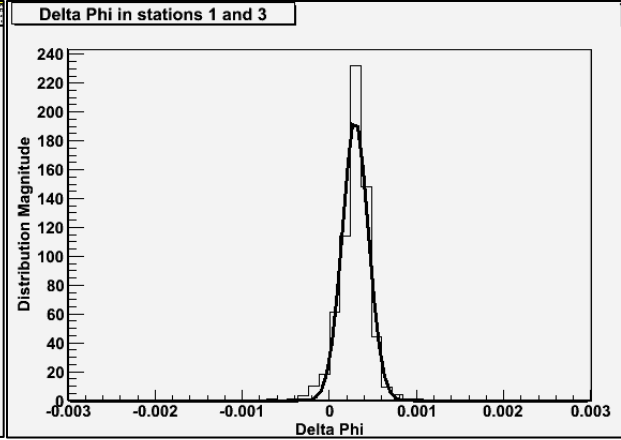


Figure 10:  $\Delta \phi$  between stations 1 and 3

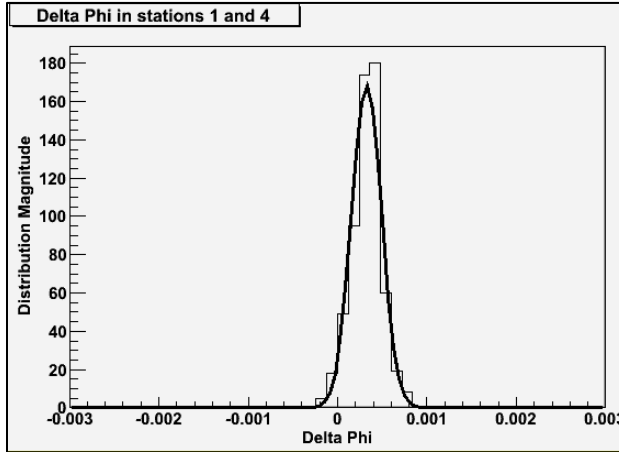


Figure 11:  $\Delta \phi$  between stations 1 and 4

This process was continued for a range of Pt between 300 GeV and 1 TeV. These plots were fit with a Gaussian distribution, and then the means and were recorded. Table 1 shows the recorded values.

	<u>Station 1 &amp; 2</u>		<u>Station 1 &amp; 3</u>		<u>Station 1 &amp; 4</u>	
	Mean	Sigma	Mean	Sigma	Mean	Sigma
1 TeV/c (neg)	-1.6862	1.2248	-2.8846	1.2598	-3.7406	1.3878
750 GeV/c (pos)	2.3106	1.4568	3.7928	1.4780	4.4262	1.7223
750 GeV/c (neg)	-2.2478	1.2905	-3.9521	1.2872	-4.5771	1.6393
500 GeV/c (pos)	3.1163	1.6742	5.5323	2.6281	6.0268	2.7517
500 GeV/c (neg)	-3.1023	2.1745	-5.4640	2.5803	-6.1845	2.8404
300 GeV/c (pos)	5.1698	2.8563	8.0588	3.8497	8.9086	4.6329
300 GeV/c (neg)	-5.2535	2.5758	-8.9192	3.0641	-10.3151	3.1794

Table 1: Recorded  $\Delta \phi$  values

Data from Table 1 was then imported into a plot. Figure 12 shows  $\Delta \phi$  as a function of momentum from 300 GeV to 1 TeV. The blue fit corresponds to detections between stations 1 and 2, the red fit corresponds to detections between stations 1 and 3, and the black fit corresponds to detections in between stations 1 and 4.

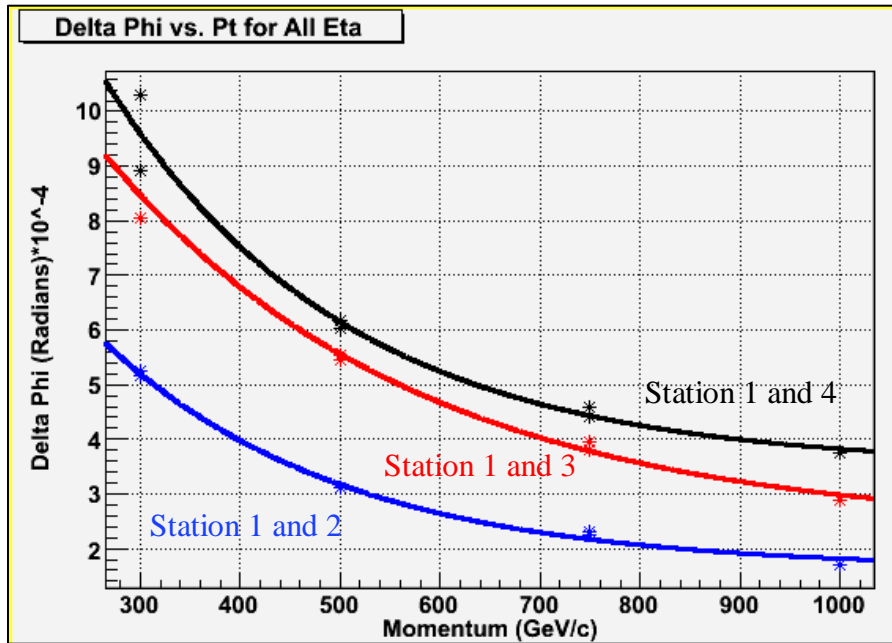


Figure 12:  $\Delta \phi$  vs. Pt

As one can see, the bending increases as you increase the in station for all Pt studied. Moreover, as the Pt increases, the bending decreases. This is intuitively sound because the less momentum the more likely to be deflected. The above data was fit with an exponential plus a constant. The values for the fit constants were:

$$\text{Station 1 and 2: } \Delta \phi = 12.5645e^{-0.00419 Pt} + 1.62421$$

$$\text{Station 1 and 3: } \Delta \phi = 16.1286e^{-0.00322 Pt} + 2.33785$$

$$\text{Station 1 and 4: } \Delta \phi = 21.3715e^{-0.00417 Pt} + 3.49517$$

Figures 9 through 12 are for all  $\eta$ ; however, it is necessary that we see how  $\Delta \phi$  behaves as  $\eta$

changes. Because any absolute value of  $\eta$  larger than one will not register in the DTs, we looked at eta in a 0.25 wide span between -1.0 and 1.0 to see how the delta phi plots changed with eta.

Figures 13, 14, and 15 show the difference  $\eta$  makes on each of the stations compared.

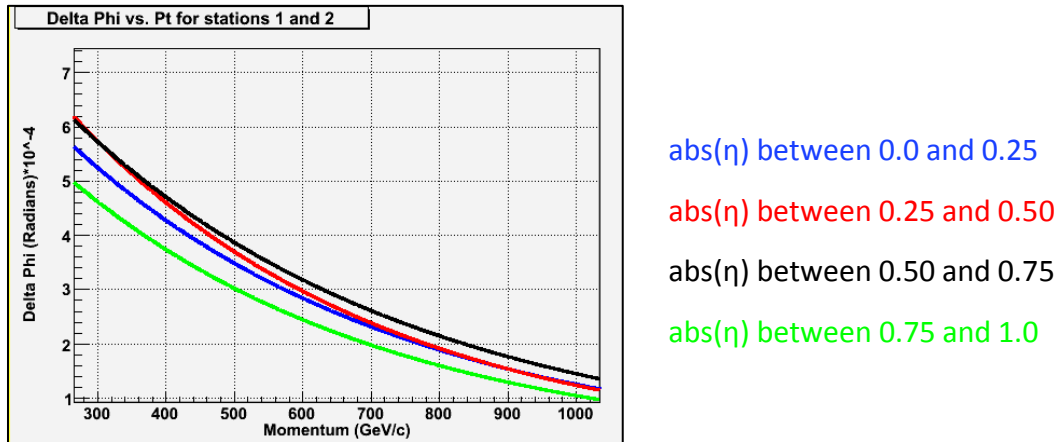


**Figure 13:  $\Delta \phi$  between stations 1 and 2**

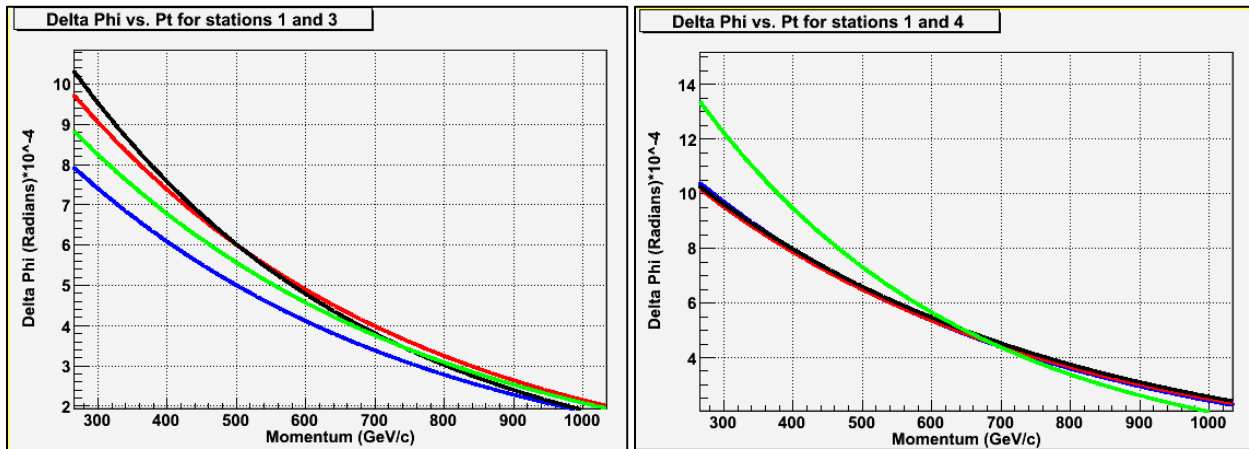


**Figure 14:  $\Delta \phi$  between stations 1 and 3**

**Figure 15:  $\Delta \phi$  between stations 1 and 4**

Figures 13-15 were plotted using absolute value of  $\eta$  due to the symmetry of the detector. If any effects are present,  $\eta$  between -0.25 to 0.0 and 0.0 to 0.25 will register the same effects on the muon.

## Conclusion:

Energies at the LHC will provide a closer look into physics at the sub-atomic level. These new energies bring by-products previously unaccounted for such as muon showering. Our algorithm produces accurate muon reconstruction regardless of a shower present. For measuring  $\Delta\phi$  using this algorithm, an exponential plus a constant provides a good fit for the extracted data. For future studies, implementing this algorithm for the CSCs will increase their usability. CSC analysis will provide data on  $\eta$  values larger than 1.0 and less than -1.0. Once this is completed, future study on the performance and efficiency of the algorithm would be allow one to see how well this method compares to previous muon reconstructing methods.

## Acknowledgments:

I would like to thank Dr. Ivan Furic for his patience, encouragement, and advisement throughout this program. I would also like to thank all those in the graphics lab who helped with all my programming and software issues. This REU program has not only taught me how to do active research and present one's findings, but it also has introduced me to a number of topics on the forefront of current research in physics. For this I want to thank all those who were able to take their time and present to the REU students these current topics. Finally, thanks to Dr. Selman Hershfield and the NSF for allowing me to participate in this invaluable research experience.

## References:

- [1] J. G. Layter, *CMS Muon Technical Design Report*, 1997, pp. 1-19, 48.
- [2] CMS Collaboration, <http://cms.cern.ch/>.
- [3] H. Bichsel, D.E. Groom, and S.R. Klein, *Passage of particles through matter*, (2005)